

CHAPTER II

Preparation of Ferrites and
X-ray Diffractometry

In this chapter the actual method of preparation of the ferrite system under investigation has been presented in article (2.1). The method of preparation employed is standard ceramic technique. All the steps that follow in this method are given together with the explanation for stoichiometric and non-stoichiometric compositions and heat treatment. The x-ray diffractometry of the ferrite samples was done by employing cobalt target using filtered Co-K α radiations. However, the diffractometry was done for only slow cooled samples. In articles (2.2) onwards the general methods of x-ray diffraction are explained, the emphasis being given on Powder Method and the principle of diffractometry. The method of indexing is explained and the crystallographic results on the samples studied are presented.

2.1 PREPARATION OF FERRITES

2.1A. General Formula :

The ferrite system selected for study is $\text{Cu}_x \text{Fe}_{3-x} \text{O}_4$ where $x = 1, 0.8, 0.6, 0.4$ and 0.2 .

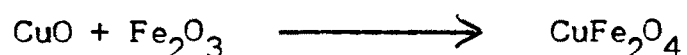
2.1B. Raw Materials :

Pure oxides CuO and Fe_2O_3 were supplied by Riddle Heiag Seize Honouer Germany.

2.1C. Nonstoichiometry :

As is mentioned in chapter 1, article (1.2), the electrical

neutrality is achieved by way of stoichiometric proportions of the ingredients. One of the samples prepared this way is simple copper ferrite i.e. CuFe_2O_4 . The other samples do not balance the electric charge equality between anions and cations. However, the single phase homogenous compound with spinel structure can be obtained. This is done in the following way.



x	Molecular Weight of CuO.	Molecular Weight of Fe_2O_3
1	79.550 gms	159.70 gms
0.8	63.642 gms	175.67 gms
0.6	47.724 gms	191.64 gms
0.4	31.816 gms	207.61 gms
0.2	15.908 gms	223.58 gms

In order to prepare a sample with formula $\text{Cu}_{0.2}\text{Fe}_{2.8}\text{O}_4$, the accurately weighed oxide powders CuO (15.908 gms) and Fe_2O_3 (223.58 gms) can be mixed.

2.1D Mixing of Oxides :

A semi-microbalance was used to weigh the oxides accurately. The fine powders of oxides, in proper molar proportions, were dry mixed. Each dry mixture of oxides was mixed thoroughly and a paste was prepared in an agate mortar using acitone for homogeneity. The mixtures were dried in the atmosphere and were transferred into platinum crucibles covered with lids.

2.1E Pre-sintering :

The mixtures in crucibles were heated in a glowbar furnace by increasing the temperature of the furnace upto 700°C . The temperature of the furnace at 700°C was maintained steady continuously for 10 hours. The samples were furnace cooled by switching off the furnace current. The calibrated Al-Cr thermocouple and a D.R. potentiometer were used for the measurement of temperature of the furnace.

2.1F Milling :

The presintered samples taken out of the crucibles were ball-milled in alcohol medium for two hours. The samples were again transferred to platinum crucibles.

2.1G Calcination to Final Product :

The same samples were calcinated to achieve their final products. The temperature of the furnace was increased slowly upto 950°C and was maintained constant for 40 hours continuously. The 40 hours duration is reported to be necessary and sufficient period for the completion of solid state reaction.¹ The samples were later slowly cooled by decreasing the current of the furnace.

1.1H Remilling :

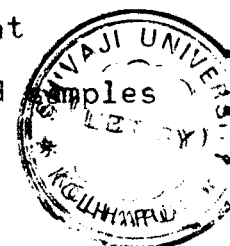
The final products thus obtained were milled and ground in a ball mill with the alcohol medium for three hours. The material in a powder form was well collected in specified dry bottles.

2.1I Pressing to Shape (Pellets) :

All the ferrite powders were sieved by a sieve particle size of 28 micron. One gram of the sample was taken in a agate mortar and mixed with polyvenyl acetate (PVA) as a binder. The powder was mixed thoroughly. The dry powder was completely transferred to a clean die of one centimeter diameter. The cold pressing in a hydraulic press was made by applying more than 10 tonnes per square inch for 10 minutes. The pellets of each composition were thus collected in required numbers.

2.1J Final Sintering and Quenching of the Pellets :

One sample of each composition was required to be quenched at different temperatures i.e. at 800°C, 600°C and 400°C; and one sample each to be slow cooled. Therefore four pellets of each composition were prepared and introduced into the furnace. The temperature of the glow bar furnace was raised slowly and maintained constant at 950°C for more than 20 hours. The binder PVA evaporates at about 250°C and further sintering of the well pressed pellet reduces the porosity thereby shrinkage of the pellets take place. Now, the temperature of the furnace was slowly reduced at the rate of about 40°C per hour and thus was brought down to 800°C. It was maintained steady at this temperature for about one hour; then each pellet of each composition was taken out of the furnace in the atmosphere and thus air quenched from 800°C. The same procedure was repeated to obtain the air quenched samples of different compositions at different temperatures. The slow cooled samples



were collected after 24 hours after the furnace was switched off and the room temperature was reached.

To make the opposite faces of pellets parallel and smooth, the pellets were polished on polishing machine. To provide good electrical contacts, silver paste was applied on the opposite faces of each pellet.

2.2 X-RAY DIFFRACTION STUDY

2.2A Conditions and Directions of Diffraction :

The diffraction occurs only when the wave length of the wave motion equals the magnitude of the repeated distance between scattering centres. This fulfilment can be achieved following the Bragg law .

$$n\lambda = 2d' \sin\theta \quad \dots (2.1)$$

d' being the interplanar distance.

$$\therefore n\lambda < 2d' \quad \dots (2.2)$$

$$(\because 0 \leq \sin\theta \leq 1)$$

In diffraction, the least value of n being unity, the condition met at any observable angle 2θ is

$$\lambda < 2d' \quad \dots (2.3)$$

Rewriting the Bragg's law,

$$\lambda = 2 \cdot \frac{d'}{n} \cdot \sin\theta \quad \dots (2.4)$$

The coefficient of λ being unity, a reflection of any order can be conveniently considered as the first order reflection from planes real or imaginary, spaced at a distance $\frac{1}{n}$ of the previous spacing. Replacing conveniently, $d = d'/n$, we have

$$\lambda = 2d \sin\theta \quad \dots (2.5)$$

The application of the law is illustrated in fig (2.1). The number of whole wavelengths lying in the path difference between rays scattered by adjacent (hkl) planes is known as the order of diffracted beam. Fig. (2.1a) depicts the second order 100 reflection. If there is no real plane midway between the (100) planes, it can be imagined as in fig (2.1b) forming first order reflection from adjacent (200) planes. In the same way 300, 400 etc. reflections may be equivalent to the third, fourth, etc. orders from the (100) planes.

Thus, the n^{th} order reflection from (hkl) planes of spacing d' may be viewed as a first order reflection from (nh nk nl) planes of spacing $d = d'/n$. This suits with the definition of Miller indices, since (nh nk nl) indicate the Miller indices of planes parallel to the (hkl) planes with $1/n$ spacing of the latter.

The number of diffraction directions $2\theta_1, 2\theta_2, 2\theta_3$, etc. can be traced and photographed from the (100) planes by using a monochromatic incident beam at the angle $\theta_1, \theta_2, \theta_3$, etc. which produce first, second, third, etc. order reflections.

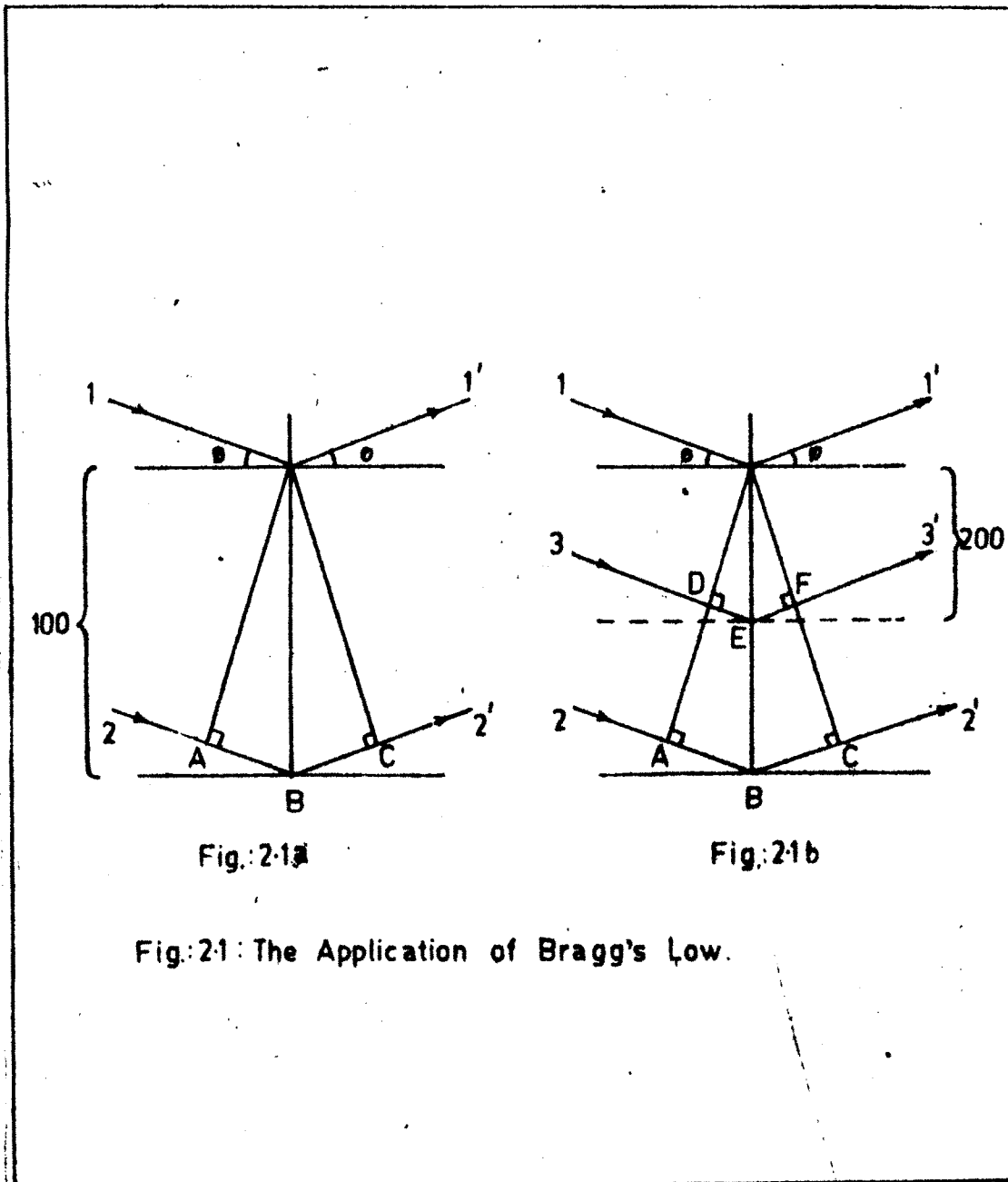


Fig:21a

Fig:21b

Fig:21: The Application of Bragg's Law.

The diffraction from other planes is also expected. The combination of Bragg law and the plane spacing expression of a particular crystal under investigation predict the diffraction angles for any set of planes.

For cubic crystal², the interplanar distance in (hkl) set of planes is

$$\frac{1}{d^2} = \frac{h^2 + k^2 + l^2}{a^2} \quad \dots \quad (2.6)$$

where a denotes the unit cell size. Combining with the Bragg's law, we have

$$\sin^2 \theta_{hkl} = \frac{\lambda^2}{4a^2} (h^2 + k^2 + l^2) \quad (2.7)$$

for known value of λ , this equation predicts all the possible Bragg angles for diffraction that occur from the planes (hkl).

If the crystal is tetragonal,² with axes a and c , the equation becomes,

$$\sin^2 \theta_{hkl} = \frac{\lambda^2}{4} \left(\frac{h^2 + k^2}{a^2} + \frac{l^2}{c^2} \right) \quad \dots \quad (2.8)$$

Thus the diffraction directions as predicted by equations (2.7) and (2.8) are determined solely by the shape and size of the unit cell. The converse of this statement is most important as far as the crystal analysis is concerned. The measurements of directions of diffracted beams speculate the shape and size of crystal's unit cell while their intensities give the information regarding the positions of atoms.

2.2B X-Ray Diffraction and Structural Analysis

The Bragg law can be utilized in the following manner :

Knowing the wavelengths λ of x-rays used and measuring various diffraction angles θ ; the interplanar distances d in a crystal can be determined. This is called the structural analysis. The structural analysis can be achieved by different diffraction methods. Diffraction occurs whenever the Bragg's law, $\lambda = 2d\sin\theta$, is satisfied. This equation imposes strict conditions on λ and θ for any crystal. The way of satisfying the Bragg condition may be achieved by varying either λ or θ during the experiment. The ways in which these quantities are varied give three main diffraction methods.

i) Laue Method³

In this method a single crystal is held stationary (θ is fixed) in the path of x-rays of continuous wavelength (λ is variable). The crystal selects out and diffracts the discrete values of λ for which the planes have interspacing d , satisfying the Bragg law. The diffraction pattern due to Laue Method consists of a series of spots. This method is convenient for the rapid determination of crystal orientation and symmetry. The Laue Method is practically never used for crystal structure determination.

ii) Rotating Crystal Method

A single crystal rotates (θ is varied) about a fixed axis in a monoenergetic beam (λ is fixed) of x-rays. The

variation in θ brings different atomic planes into position for reflection. In a course of rotation of the crystal, the beam get diffracted whenever the value of θ satisfies the Bragg equation. A modified rotating-crystal method can be used for structure determination when the available specimen is a single crystal. Several variations of the rotating-crystal method are in common use.⁴

iii) Principle of the Powder Method

The powder method of x-ray diffraction was first developed by P.Debye and P.Scherrer⁵ in 1916 and independently by A.W.Hull⁶ in 1917. This method can be used properly to get the knowledge of structural information about the sample under investigation.

In this method, the film is placed on the cylindrical surface of D.S.Camera and the specimen holder rotates about the axis of the camera in a mono-energetic beam of x-rays. The small amount of smoothly ground powder can be coated on the surface of a fine glass fibre with a glue or petroleum jelly. The specimen prepared is then mounted in its holder by proper adjustments.

The crystallites in a powder get completely randomly oriented so that the reciprocal lattice vectors of all the crystallites point in all the directions. The reciprocal lattice points lie on the surface of a sphere of radius $|\bar{\sigma}_{hkl}|$. Each reciprocal lattice sphere oriented by every possible value of σ_{hkl} cuts the Ewald's sphere. A narrow film strip (fig.2.2a,b) is used to record the representative portion of the cuts.

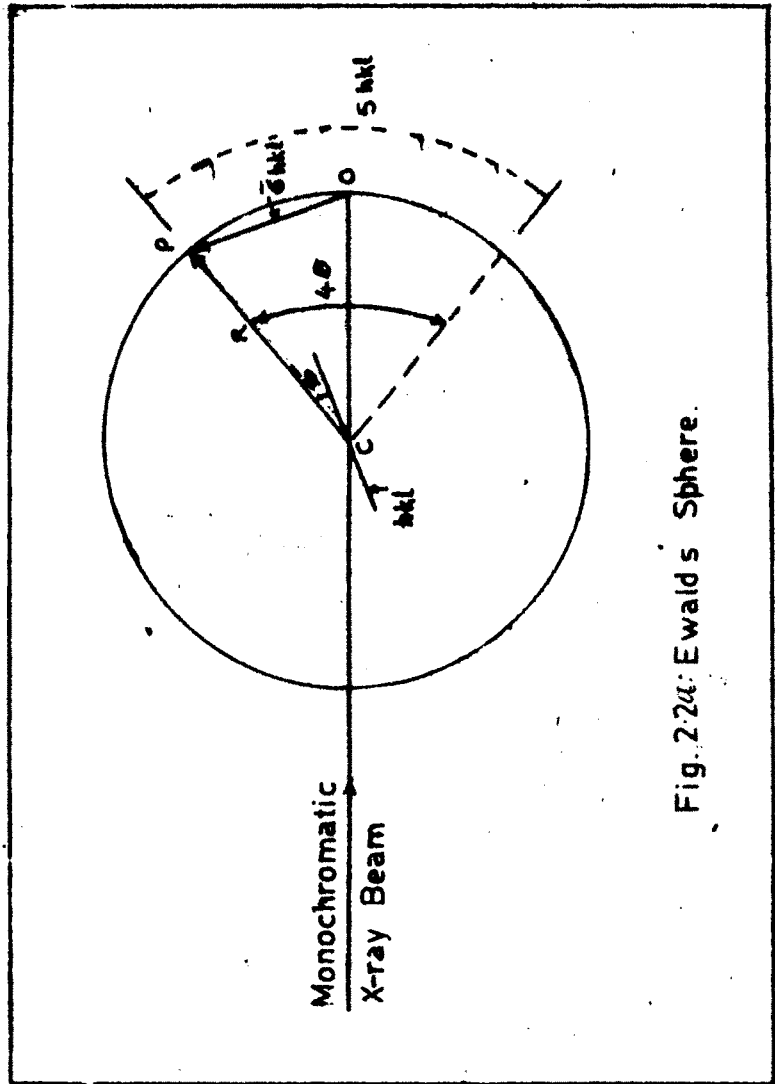


Fig. 2.2a: Ewald's Sphere.

By the geometry of Ewald's sphere,

$$4. \theta_{hkl} = \frac{S_{hkl}}{R} \dots \quad (2.9)$$

If we consider the two consecutive reflections, the angle between them is the Bragg angle which can be readily written as

$$\theta_{hkl} = \frac{S_{hkl}}{4} \dots \quad (2.10)$$

The measurements of S_{hkl} in mm. on photographic film give the values of θ_{hkl} .

Using Bragg's law,

$$2 d_{hkl} \cdot \sin \theta_{hkl} = \lambda \dots \quad (2.11)$$

the interplanar distances d_{hkl} can be determined.

2.2C X-Ray Diffractometer and its Principle

The film in a Debye-Scherrer is replaced by a movable counter in an x-ray diffractometer. The principle of the method and main features of the diffractometer are shown in fig. (2.3). The incident beam of x-rays, free from K_{α} radiations made by use of a filter is allowed to pass through the slit 'A' of the collimator. The K_{α} radiations thus fall on the sample powder kept in a holder 'C' and get reflected by crystal planes satisfying the Bragg's law. As the crystallites are randomly oriented a reflection at the particular position is due to a set of atomic planes which satisfy the Bragg's condition. The diffracted beam from the set of parallel planes of the specimen get converged and focused at a slit 'F', which further enters the counter 'G'. With the help of a special

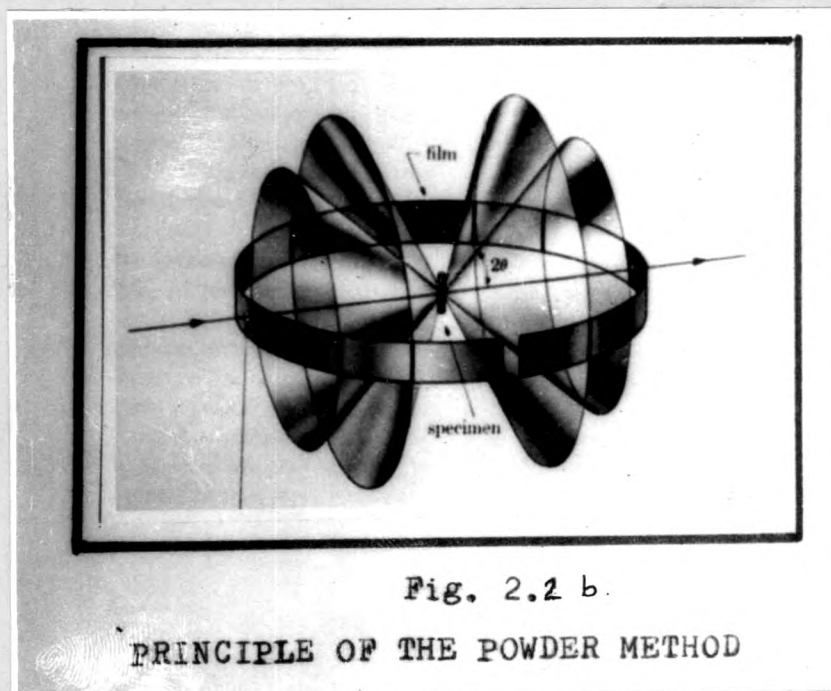


Fig. 2.2 b.

PRINCIPLE OF THE POWDER METHOD

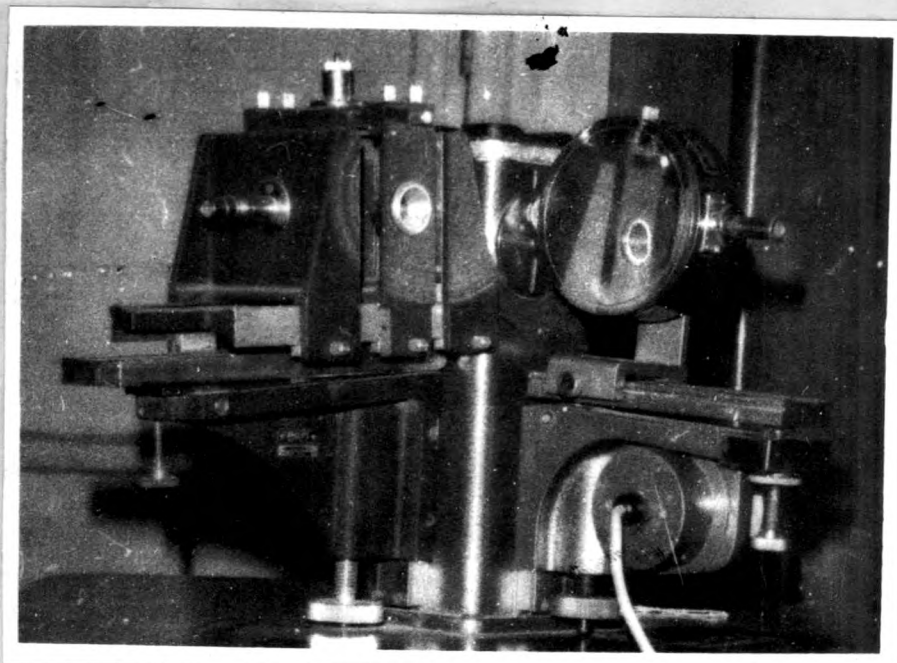


Fig. 2.3 a: Experimental set-up for X-ray diffractometer.

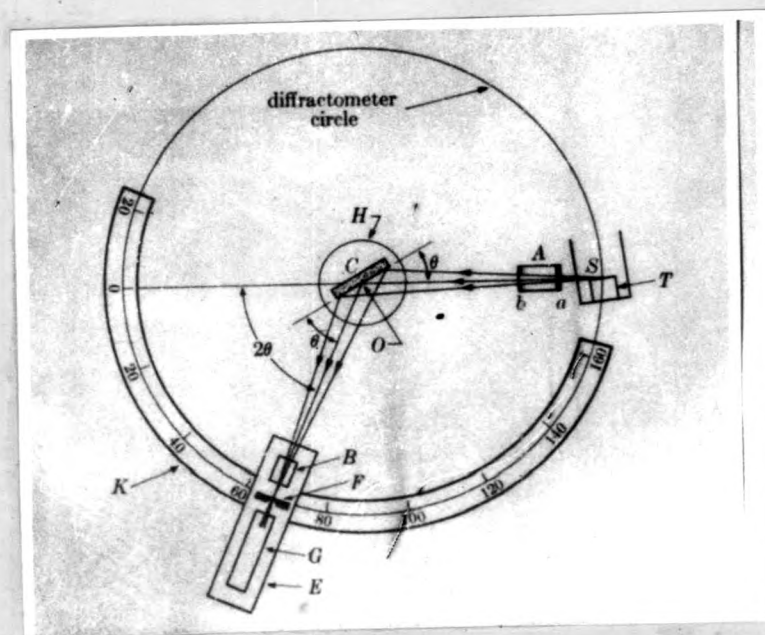


Fig.2.3 b: X-ray diffractometer (schematic).



slit 'B', the diffracted beam is collimated. The counter 'G' is connected to a counter rate-meter. The output of the circuit is fed to a fast automatic recorder which registers the counts per second versus the angle ' 2θ '. The location of the centroid of the peak registered gives the value of $2\theta_{hkl}$ for the corresponding Bragg-reflection.

The carriage 'E' supports the receiving slits and the counter. The carriage 'E' is free to rotate about an axis 'C'. The angular position ' 2θ ' of the carriage and hence that of the counter 'G' may be noted on the graduated circular scale 'K'. The mechanical coupling of 'E' and 'H' is made so that the rotation of the counter G through an angle 2θ degrees moves the specimen (C) through an angle θ degrees. It also ensures that the complimentary angles of incidence and reflection from the flat specimen are always equal to each other, each being half the total angle of diffraction. This type of arrangement is necessary to satisfy the focusing conditions. The power driven counter moves with a constant angular velocity about the axis of the diffractometer for any desired angular range from 1° to 160° . The main advantage of the diffractometer over the Debye-Scherrer powder method is that it gives a quantitative measure of the intensity.

The diffractometer records of each composition for slow cooled samples only were made on Philips X-ray diffractometer (type P.W. 1051, ~~1051~~) in T.I.F.R., Bombay. For the purpose of x-ray diffractograms, finely powdered specimen

were kept in a recess of perspex plate and compacted under sufficient pressure to form cohesion without any binder. The perspex plate with sample was inserted in the holder 'C'. Co target was used for CuFe_2O_4 and $\text{Cu}_x\text{Fe}_{3-x}\text{O}_4$ ferrites ($0 < x \leq 1$). The filtered K_α radiations from an x-ray tube operated at 30kV and 15 mA were used. By a trial method, the rate meter was adjusted so that the maximum height of the diffraction peak should lie wholly on the chart. The speed of the goniometer was kept 2 degrees per minute. The recording was done in a range 20° to 80° of 2θ . The area under the peak is proportional to the intensity of the reflection.

2.2D Indexing of the Powder Pattern :

The powder pattern of each slow cooled sample of the system $\text{Cu}_x\text{Fe}_{3-x}\text{O}_4$ ($0 < x \leq 1$) were obtained with a diffractometer. The object of scanning was kept to cover as wide range of 2θ as possible between 20° and 80° . The value of $\sin^2\theta$ was calculated for each peak observed in the pattern. The set of these $\sin^2\theta$ values is the raw material for the determination of cell size and shape.

For a cubic lattice, the relation between the interplanar distance d_{hkl} , lattice parameter a , and the indices hkl can be represented by the formula⁷

$$d_{hkl} = \frac{a}{\sqrt{h^2+k^2+l^2}} \quad \dots \quad (2.12)$$

As the peak in the diffraction pattern is obtained, the Bragg's law must be obeyed,

$$2. d_{hkl} \cdot \sin \theta_{hkl} = \lambda \quad \dots \quad (2.13)$$

combining these two equations,

$$2. \left(\frac{a}{\sqrt{h^2+k^2+l^2}} \right) \cdot \sin \theta_{hkl} = \lambda$$

$$\therefore \frac{\sin^2 \theta_{hkl}}{h^2+k^2+l^2} = \frac{\sin^2 \theta_{hkl}}{s} = \frac{\lambda^2}{4 a^2} \quad \dots \quad (2.14)$$

where, the sum $s = h^2 + k^2 + l^2$.

The sum, s , is always an integer and the value of $\lambda^2 / 4 a^2$ must be constant for any observed peak in the pattern. Thus the set of integers s should be selected properly to yield a constant quotient when divided one by one into the observed $\sin^2 \theta$ values. Rearranging the equation (2.14) as

$$\sin^2 \theta_{hkl} = \frac{\lambda^2 s}{4 a^2} \quad \dots \quad (2.15)$$

we find that the quantity $\lambda^2 / 4a^2$ is the greatest common factor (GCF) in $\sin^2 \theta$. As a first step GCF was determined from a few lines at the lower angles and then all the other proper integers were found. Once the integers s were known, the indices hkl of reflecting plane were written down by inspection. When a set of integers satisfying equation (2.14) were not found, the other possible tetragonal system was checked and found in good agreement.

For a tetragonal unit cell⁷ the relation can be written as

$$d_{hkl} = \left(\frac{h^2+k^2}{a^2} + \frac{l^2}{c^2} \right)^{-1/2} \dots \quad (2.16)$$

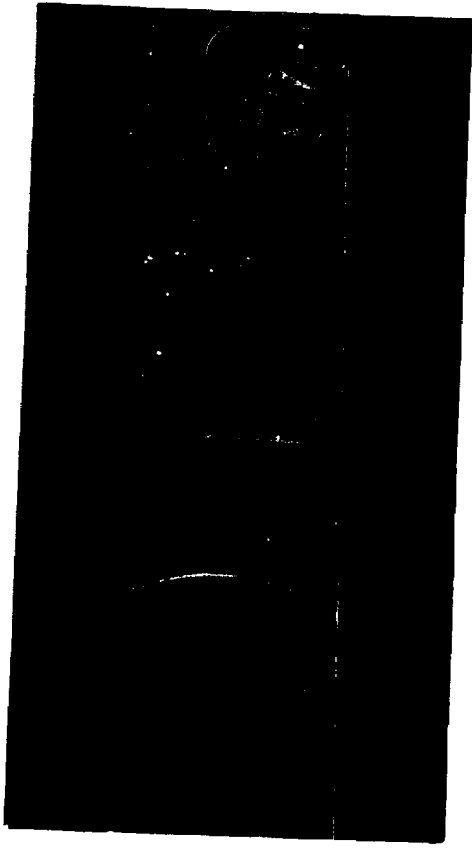
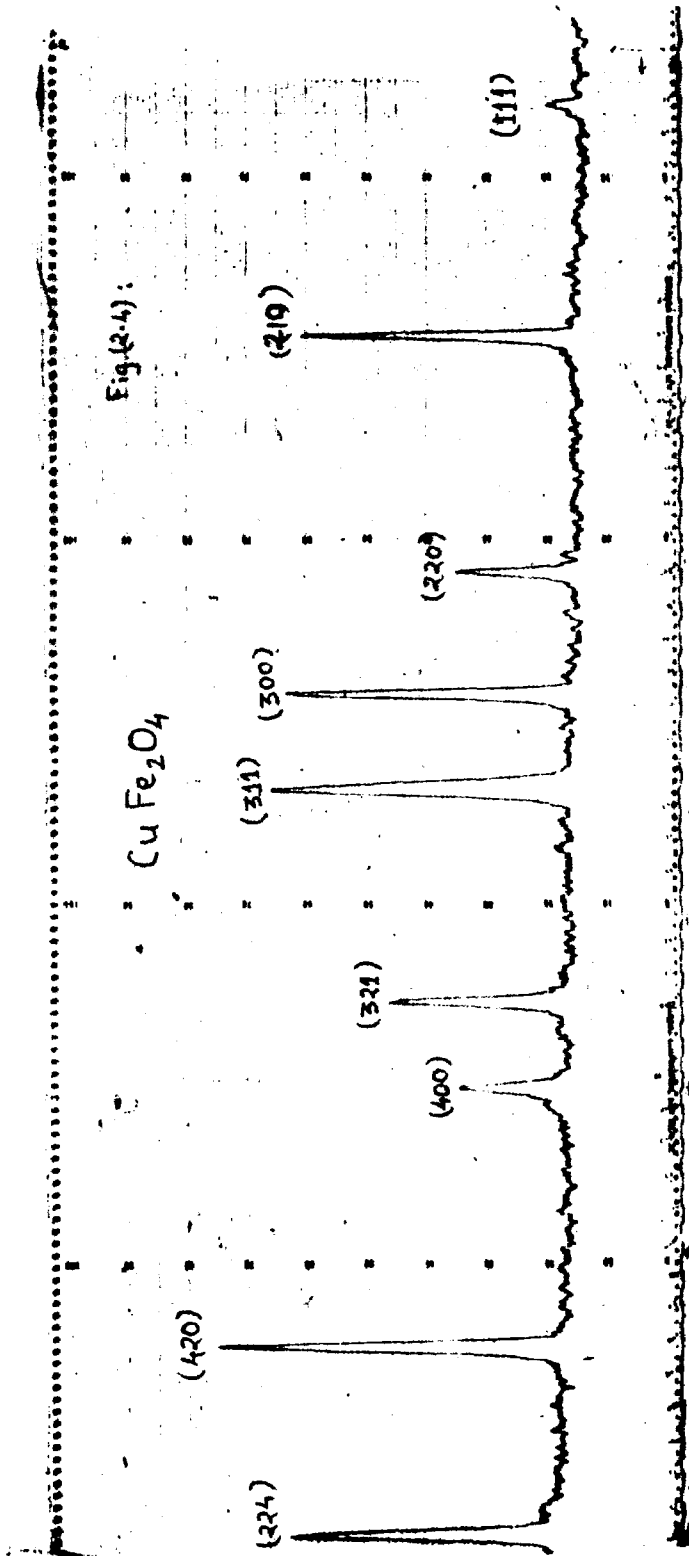
where 'a' and 'c' are the lattice parameters. Combining this with Bragg's relation, we get,

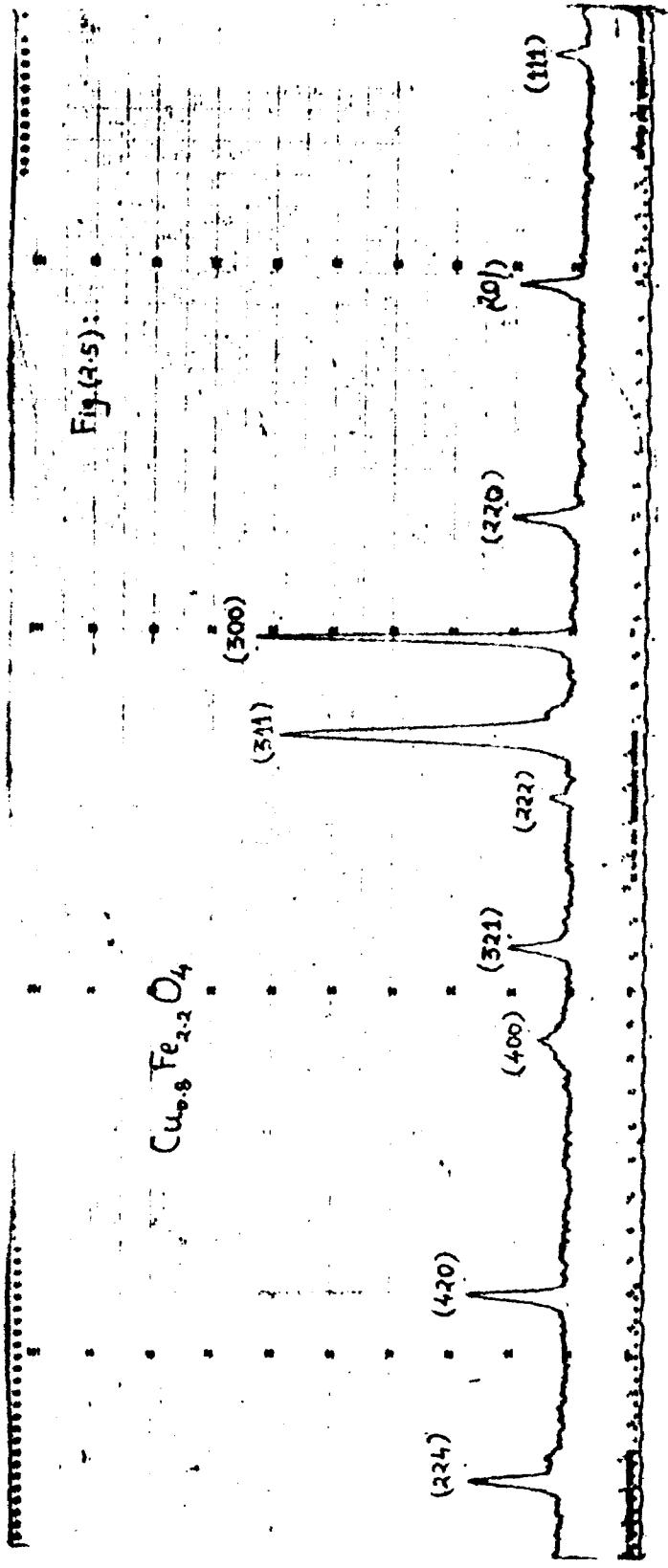
$$\sin^2 \theta_{hkl} = \frac{\lambda^2}{4} \left(\frac{h^2+k^2}{a^2} + \frac{l^2}{c^2} \right) \dots \quad (2.17)$$

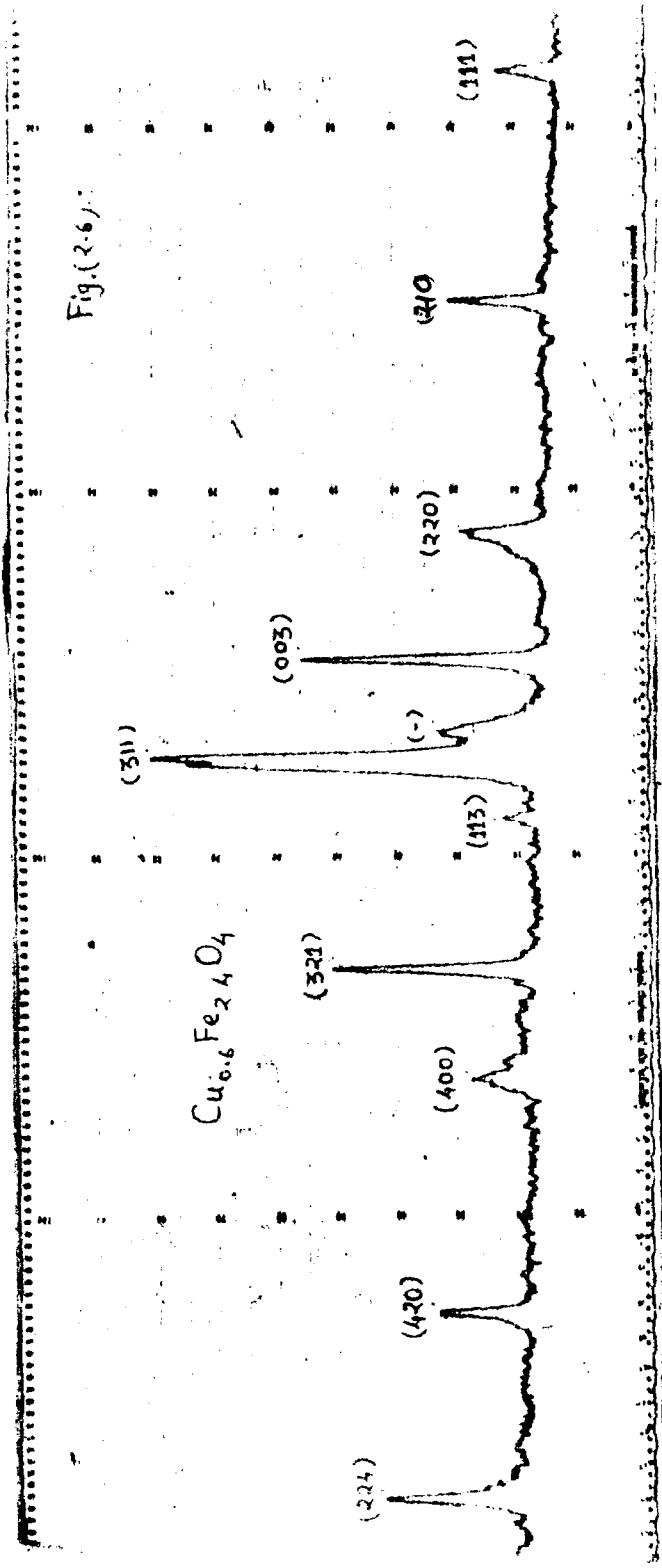
$$\text{or } \sin^2 \theta_{hkl} = A (h^2 + k^2) + C \cdot l^2 \dots \quad (2.18)$$

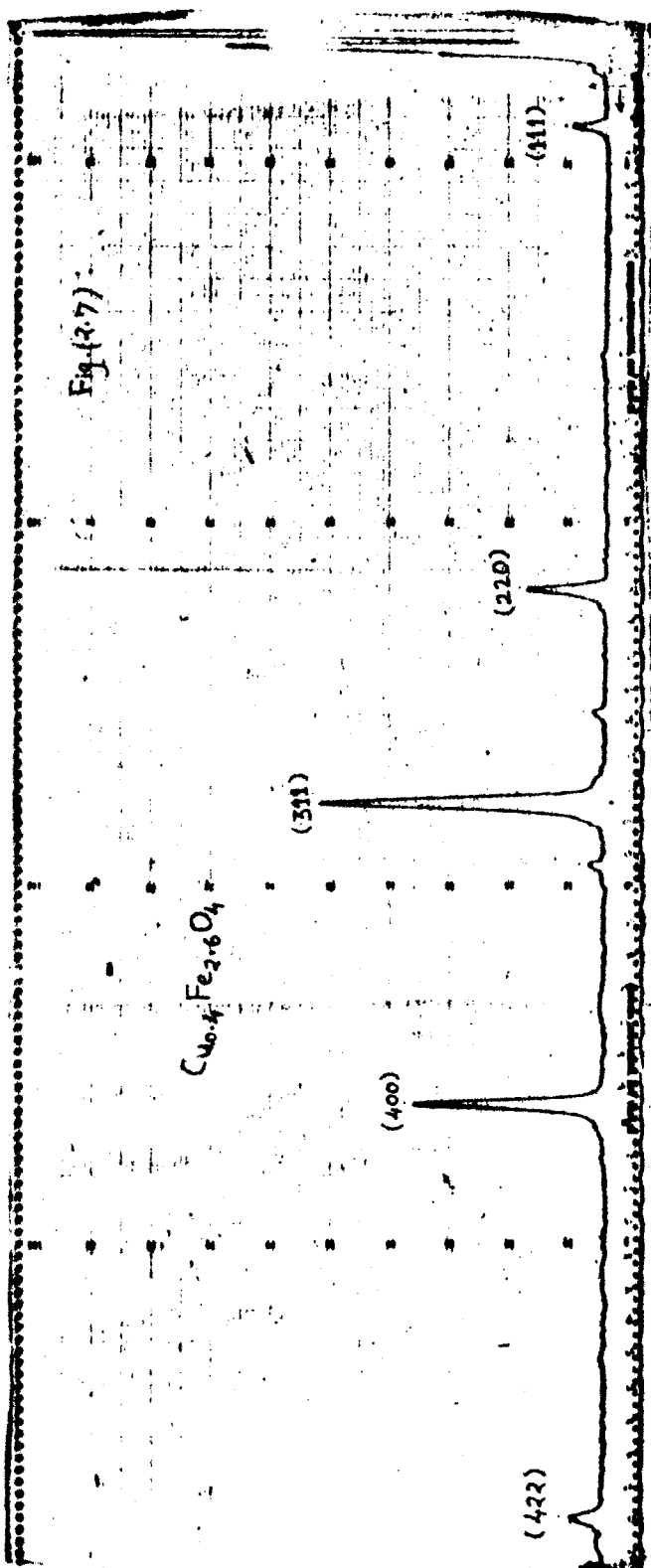
$$\text{where } A = \lambda^2 / 4a^2 \text{ and } C = \lambda^2 / 4c^2 \dots \quad (2.19)$$

For crystals having tetragonal symmetry the patterns are more complicated. The simplest analytical method to index such a pattern is to find relationships between the values of $\sin^2 \theta$ which yield an indication of the crystal symmetry. The value of the factor A was computed by using equation (2.19) for $l = 0$. The allowed values of (h^2+k^2) are 1, 2, 4, 5, 8 etc. Thus the hko lines must have the values of $\sin^2 \theta$ in the ratio of these integers where A will be some number $1, \frac{1}{2}, \frac{1}{4}, \frac{1}{5}, \frac{1}{8}$ etc., times the values of $\sin^2 \theta$ of these peaks in the pattern. Substituting the values of A in equation (2.18) for known values of $\sin^2 \theta$ with $l = 1, 2, 3$, the factor C was determined. Making use of these common factors, all the reflections were indexed. The lattice parameter 'a' was obtained from the reflections for which $l=0$. Substituting this value of 'a' for reflections at higher angles, the value of 'C' was calculated.









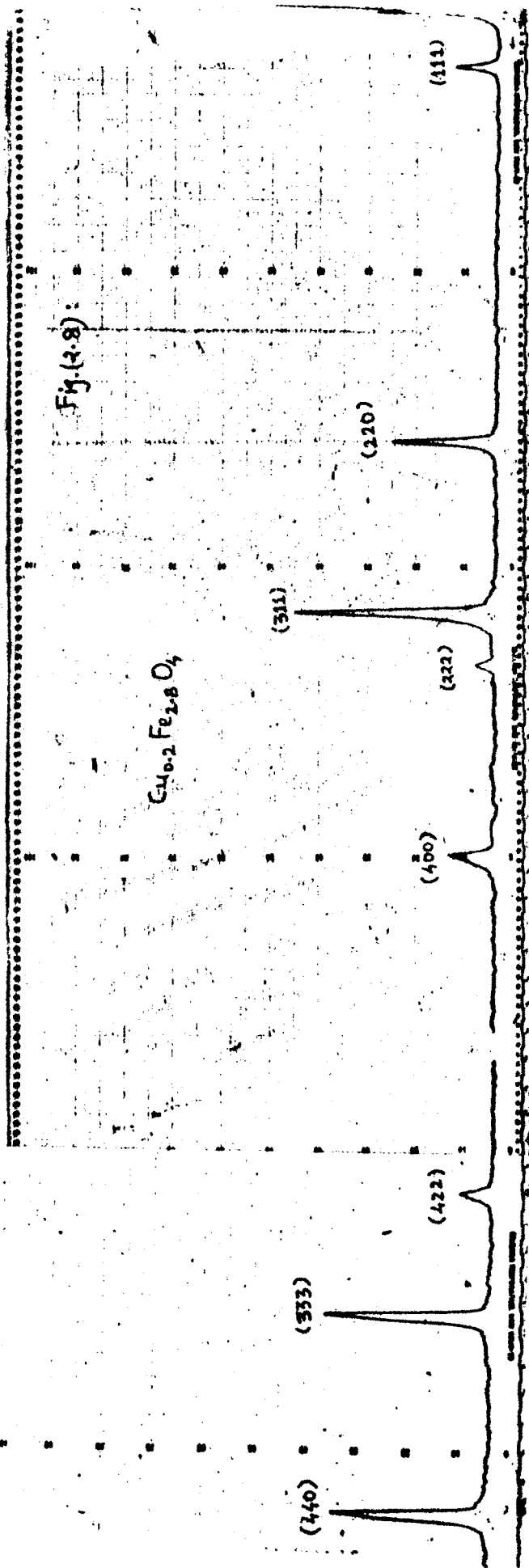


TABLE NO. 2.1

DATA ON CRYSTAL STRUCTURE OF $\text{Cu}_x\text{Fe}_{3-x}\text{O}_4$ FERRITESAMPLE : CuFe_2O_4

x = 1.0

hkl	d in Å° Observed	d in Å° Calculated	Lattice Constants
111	4.8434	4.9010	
210	3.6999	3.7466	
220	2.9767	2.9619	a = 8.3775 Å°
300	2.7015	2.7925	c = 8.7256 Å°
311	2.5265	2.5349	
321	2.2314	2.2453	$\therefore \frac{c}{a} = 1.0415$
400	2.1023	2.0944	
420	1.8580	1.8733	
224	1.7456	1.7564	
422	1.7958	1.7213	
115	1.6435	1.6740	
511	1.6196	1.6145	
-	1.6007	-	
440	1.4908	1.4809	
530	1.4555	1.4367	

TABLE NO. 2.2DATA ON CRYSTAL STRUCTURE OF $\text{Cu}_x\text{Fe}_{3-x}\text{O}_4$ FERRITESAMPLE : $\text{Cu}_{0.8}\text{Fe}_{2.2}\text{O}_4$ $x = 0.8$

hkl	d in A° Observed	d in A° Calculated	Lattice Constants
111	4.8210	4.8111	
201	3.6871	3.7251	
220	2.9767	2.9432	$a = 8.3247 \text{ A}^\circ$
300	2.7015	2.7749	
311	2.5265	2.5107	$c = 8.3500 \text{ A}^\circ$
222	2.4209	2.4055	
321	2.2094	2.2253	$\therefore \frac{c}{a} = 1.0030$
400	2.1023	2.0812	
420	1.8463	1.8615	
224	1.6962	1.7027	
511	1.6154	1.6023	
115	1.6007	1.6066	
440	1.4839	1.4716	
530	1.4539	1.4276	

TABLE NO. 2.3

DATA ON CRYSTAL STRUCTURE OF $\text{Cu}_x\text{Fe}_{3-x}\text{O}_4$ FERRITESAMPLE : $\text{Cu}_{0.6}\text{Fe}_{2.4}\text{O}_4$ $x = 0.6$

hkl	d in \AA° Observed	d in \AA° Calculated	Lattice Constants
111	4.8210	4.8066	
210	3.6742	3.7784	
220	2.9849	2.9874	$a = 8.4488 \text{ \AA}^{\circ}$
003	2.6948	2.6979	$c = 8.0939 \text{ \AA}^{\circ}$
-	2.5619	-	
311	2.5207	2.5371	$\therefore \frac{c}{a} = 0.9579$
113	2.4208	2.4588	
321	2.2050	2.2508	
400	2.1023	2.1122	
420	1.8405	1.8892	
224	1.6962	1.6753	
115	1.6132	1.5624	
511	1.5965	1.6022	
440	1.4891	1.4936	
530	1.4555	1.4489	

TABLE NO. 2.4

DATA ON CRYSTAL STRUCTURE OF $\text{Cu}_x\text{Fe}_{3-x}\text{O}_4$ FERRITESAMPLE : $\text{Cu}_{0.4}\text{Fe}_{2.6}\text{O}_4$ $x = 0.4$

hkl	d in A° Observed	d in A° Calculated	Lattice Constants
111	4.8434	4.8508	
220	2.9767	2.9705	a = 8.401 A°
311	2.5323	2.5332	
400	2.1022	2.1005	
422	1.7156	1.7150	
333	1.6154	1.6169	
440	1.4839	1.4853	

TABLE NO. 2.5

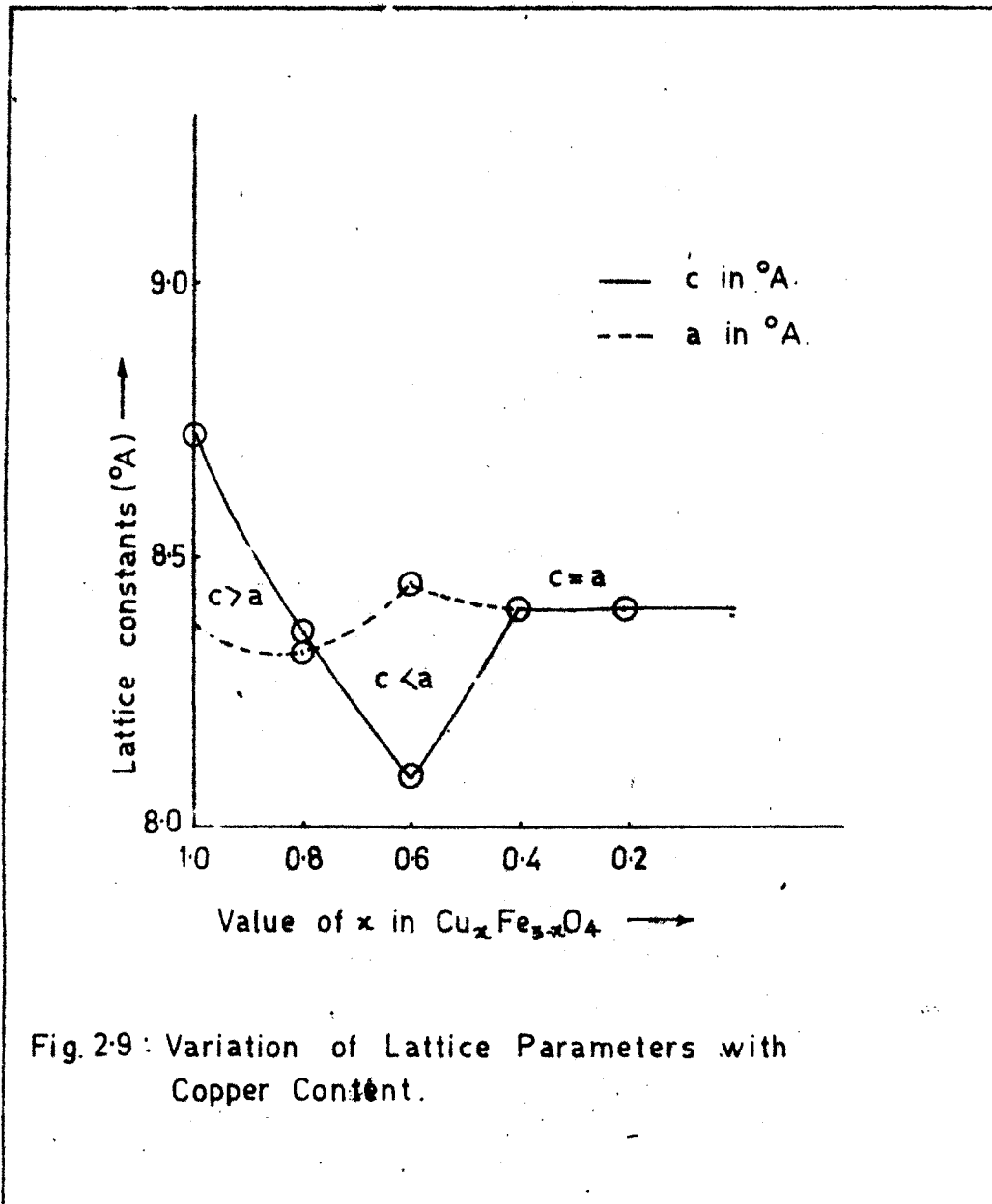
DATA ON CRYSTAL STRUCTURE OF $\text{Cu}_x\text{Fe}_{3-x}\text{O}_4$ FERRITESAMPLE : $\text{Cu}_{0.2}\text{Fe}_{2.8}\text{O}_4$ (x = 0.2)

hkl	d in A° Observed	d in A° Calculated	Lattice Constants
111	4.8434	4.8551	
220	2.9767	2.9731	a = 8.409 A°
311	2.5382	2.5355	
222	2.4262	2.4276	
400	2.1023	2.1023	
422	1.7156	1.7165	
333	1.6175	1.6184	
440	1.5031	1.4866	

2.3 RESULTS AND DISCUSSIONS

The diffractometric records of slow cooled $\text{Cu}_x\text{Fe}_{3-x}\text{O}_4$ samples only were obtained and the same are shown in Figs. (2.4 to 2.8). The diffraction maxima were indexed by GCE method as explained elsewhere and were checked and tallied with those expected for spinel structure^{2,8}. The reflections observed in cubic structure are (111), (220), (311), (222), (400), (422), (333) and (440) and for tetragonal structure the planes observed are (111), (220), (300), (311), (222), (321), (400), (420), (224), (511), (115), (440) and (530). These planes are allowed for spinel structure. The d values of $\text{Cu}_x\text{Fe}_{3-x}\text{O}_4$ samples for $x = 1.0, 0.8, 0.6, 0.4,$ and 0.2 are represented in tables (2.1 to 2.5). The calculated d values of the samples are in close agreement with the observed 'd' values. The lattice parameters 'a' and 'c' were determined for different compositions of the system. Fig. (2.9) shows the variation of lattice parameters (a or c) with the percentage decrease of Cu^{+2} . It is observed that with decrease of Cu^{+2} content, both c and a values decrease and then increase to give c/a ratio to be unity. This behaviour clearly indicates that the ratio c/a is either greater or less than unity. When the value of c/a ratio becomes unity the system forms cubic structure.

The systems CuFe_2O_4 , $\text{Cu}_{0.8}\text{Fe}_{2.2}\text{O}_4$ and $\text{Cu}_{0.6}\text{Fe}_{2.4}\text{O}_4$ show tetragonal structures while the systems $\text{Cu}_{0.4}\text{Fe}_{2.6}\text{O}_4$ and $\text{Cu}_{0.2}\text{Fe}_{2.8}\text{O}_4$ show the cubic structure.



The axial ratio c/a for slow cooled CuFe_2O_4 is reported to be varying from 1.03 to 1.06⁹⁻¹². Our value of c/a i.e. 1.04 for slow cooled CuFe_2O_4 lie within a range of this reported values.

Copper ferrite exhibits tetragonal structure at lower temperature and cubic at higher temperature. The transition temperatures are also reported^{9,11-14}. The tetragonal distortion of the spinel lattice is generally accepted as the result of sufficient concentration of distorting Cu^{+2} ions on the octahedral sites (B-sites) of the lattice and the orientation of the oxygen octahedra distorted by Cu^{+2} ions throughout the crystal. The inverse character of copper spinel changes to normal form as the temperature increases. When 75 % Cu^{+2} ions lie on B sites the partially inverted structure exhibits a cubic lattice instead of tetragonal^{14,15}.

2.4 REFERENCES

1. R.G.Kulkarni, V.U.Patil : J.Mat.Sci. 15 (1980) 2221.
2. B.D.Cullity : "Elements of x-ray Diffraction" Addison-Wesley Publishing Co.INC-England (1959).
3. A.Taylor : "X-Ray Metallography" John Wiley and Sons, Inc. New York. (1961).
4. C.Kittel : "Introduction to Solid State Physics" 3rd Edn. Wiley Eastern Private Ltd., New Delhi.
5. P.Debye and P.Scherrer : Physik.Z. 17,277 (1916) and 18, 219 (1917).
6. A.N.Hull : Phys.Rev., 9, 84, 564 (1916) and 10,661 (1917).
7. Henry,N.F.M., Lipson,H. and Wooster,W.A. : The interpretation of x-ray diffraction photographs. Macmillan and Co. Ltd., London (1961).
8. F.C.Phillips : "An Introduction To Crystallography" Longmans, Green and Co., Ltd., London, 1949.
9. Prince,E., Treuting,R.G. : Acta Crystallographica, 9,(1956), 1025.
10. Sagal,K., Tabellen,F. Rontgenstruckturanalyse, Springer, Berlin (1958).
11. Bertant,E.F., J.Phys.Rad 12 (1951), 252.
12. Borisenko,A., Toropov,N.A., Z.prikl chim. 23 (1950), 1165.

13. Weil,L., Bertant,F., Bochirol,L. J.Phys.Rad. 11 (1950),
208.
14. Ohinishi,H., Teranishi,T., Miyahava,S.J. Phys.Soc.Japan,
14 (1959), 106.
15. Finch,A.I., Sinha, A.P.B., Sinha,K.P. : Proc.Royal Soc.
London, A 242 (1957), 28.